Exploration of the Potential Energy Surfaces, Prediction of Atmospheric Concentrations, and Prediction of Vibrational Spectra for the $HO_2\cdots(H_2O)_n$ ($n = 1-2$) Hydrogen Bonded Complexes

Kristin S. Alongi,[†] Theodore S. Dibble,*[,‡] George C. Shields,*[,†] and Karl N. Kirschner*[,†]

Department of Chemistry, Hamilton College, Clinton, New York 13323, and Chemistry Department, SUNY-ESF, Syracuse, New York 13210

Received: December 8, 2005; In Final Form: January 25, 2006

The hydroperoxy radical (HO_2) plays a critical role in Earth's atmospheric chemistry as a component of many important reactions. The self-reaction of hydroperoxy radicals in the gas phase is strongly affected by the presence of water vapor. In this work, we explore the potential energy surfaces of hydroperoxy radicals hydrogen bonded to one or two water molecules, and predict atmospheric concentrations and vibrational spectra of these complexes. We predict that when the HO_2 concentration is on the order of 10^8 molecules·cm^{-3} at 298 K, that the number of $HO_2\cdots H_2O$ complexes is on the order of 10^7 molecules·cm^{-3} and the number of $HO_2\cdots(H_2O)_2$ complexes is on the order of 10^6 molecules·cm^{-3}. Using the computed abundance of $HO_2\cdots H_2O$, we predict that, at 298 K, the bimolecular rate constant for $HO_2\cdots H_2O + HO_2$ is about 10 times that for $HO_2 + HO_2$.

Introduction

The hydroperoxy radical (HO_2) is a molecule that is of interest in many fields, including environmental chemistry, astrochemistry, and biochemistry. It plays a significant role in Earth's atmospheric chemistry as a component of several important gas-phase reactions. The formation of the hydroperoxy radical stems primarily from the OH radical-initiated degradation of organic compounds, and the subsequent photolysis of aldehydes:[1]

$$H_2CO(g) + h\nu\ (\lambda \leq 370\ \text{nm}) \rightarrow HCO(g) + H(g) \quad (1)$$

$$H(g) + O_2 \rightarrow HO_2(g) \quad (2)$$

$$HCO(g) + O_2 \rightarrow HO_2(g) + CO(g) \quad (3)$$

The self-reaction of two hydroperoxy radicals leads to the production of molecular oxygen and hydrogen peroxide:[2]

$$HO_2(g) + HO_2(g) \rightarrow HOOH(g) + O_2(g) \quad (4)$$

Once formed, hydrogen peroxide rapidly enters aqueous aerosols where it oxidizes sulfur dioxide to sulfuric acid. The reaction of hydroperoxy radical with nitric oxide forms NO_2, whose photolysis leads to formation of ozone as shown in Scheme 1.

The hydroperoxy radical also has a very strong affinity for water. The atmospheric importance of this fact came to light 3 decades ago, when it was determined that the rate of hydroperoxy radical's self-reaction in the gas phase was strongly affected by the presence of water vapor.[2−7] This was widely suspected to result from the formation of an $HO_2\cdots H_2O$ complex, and led to one of the first ab initio studies of this hydrogen bonded complex.[8] Astronomers are also interested in understanding the interaction between hydroperoxy and water molecules as related to their interpretation of data obtained from icy surfaces in space. Radiolysis of icy surfaces on comets, interstellar dust, and satellites (e.g., Jupiter's moon Europa) could result in the chemical processes seen in hydroperoxy radical's self-reaction or its reaction with water.[9,10] The hydroperoxy radical is also believed to be important in several biological processes, where it has ample opportunity for forming weak interactions with water molecules.[11] Thus, understanding the structure and energetics of the $HO_2\cdots H_2O$ complex is fundamentally important for several fields of study.

SCHEME 1: Catalytic Cycles in HO_x and NO_x Producing Ozone While Oxidizing Volatile Organic Compounds

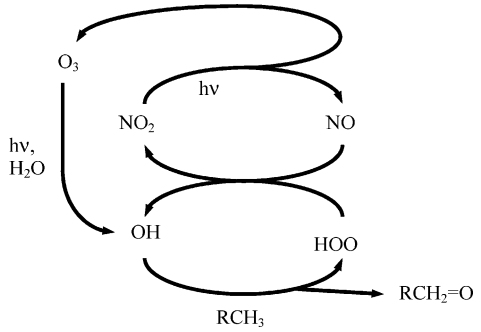

There has been an indirect determination of the equilibrium constant for formation of the $HO_2\cdots H_2O$ complex[12] and an attempt to obtain its spectrum.[13] However, no interpretable spectrum has been obtained for this complex. Recently, there have been several quantum-mechanical studies of a single conformer of the $HO_2\cdots H_2O$ complex.[14−16] Because of the role water has in hydroperoxy radical reactions, gaining a detailed energetic and structural understanding of possible $HO_2\cdots H_2O$ and $HO_2\cdots(H_2O)_2$ complexes will give additional insight into the role this hydrogen bonded system plays in atmospheric chemistry and other phenomena.

Using CCSD//MP2 calculations with a variety of basis sets, the equilibrium constant (standard state of molecule·cm^3) for reaction 5

[†] Hamilton College.
[‡] SUNY-ESF.

10.1021/jp057165k CCC: $33.50
Published on Web 02/22/2006

$$HO_2(g) + H_2O(g) \rightarrow HO_2\cdots H_2O(g) \quad (5)$$

at room temperature has been estimated to be between 4×10^{-18} and 1.3×10^{-21}.[14,17] Experimentally, Kanno and colleagues determined the reaction's equilibrium constant K_c to be $(5.2 \pm 3.2) \times 10^{-19}$ at 297 K, which leads to a concentration ratio of $[HO_2\cdots H_2O]/[HO_2]$ of 0.19 ± 0.11 at 297 K and 50% relative humidity.[12]

Hydroperoxy radical's self-reaction has been the subject of three computational studies to date,[15,18,19] two of which have examined the catalytic role of water. In addition to the $HO_2\cdots H_2O$ dimer complex, the $HO_2\cdots(H_2O)_2$ trimer is of interest. The trimer may be atmospherically relevant, and serves as a stepping stone to modeling bulk or surface hydration of HO_2.[16,20] As a model for HO_2 interacting with cloud droplets, Shi and co-workers performed quantum-mechanical calculations on the $HO_2\cdots(H_2O)_{20}$ complex.[20] They proposed that hydroperoxy radical reactions may occur on the surface and in the interior of a cloud droplet. Complexes and clusters of water with oxidants, including the hydroperoxy radical, is the subject of two recent reviews.[21,22] Our goal is to obtain all of the potential configurations of $HO_2\cdots H_2O$ and $HO_2\cdots(H_2O)_2$ complexes, and determine their energies and relative abundances in the lowermost troposphere. This is a fundamental step for obtaining a better understanding of water's role in the self-reaction of the hydroperoxy radical and its gas- and aqueous-phase chemistry.

Method

The initial $HO_2\cdots H_2O$ configurations were built using the SPARTAN[23] software by placing a water molecule about the hydroperoxy radical at three different locations. In two of these configurations, each radical oxygen atom accepted a hydrogen bond from the water, while the third configuration had the water accepting a hydrogen bond from the hydroperoxy radical. Additional configurations were generated using a 12-fold rotation around the hydrogen bond of each initial structure, and each of these configurations was optimized with PM3. The resulting conformers were grouped based on dihedrals of matching signs (positive or negative) and similar values (i.e., 0−8, 8−25, 25−90, 90−120, 120+). Previous work on small water clusters has shown that PM3 geometry optimizations of conformers with similar dihedral angles converge on a common minimum.[24] The groups were not based on energies because most conformations from each search possessed PM3 heat of formation energies within 3 kcal·mol^{-1} of each other. We performed a Hartree−Fock (HF) 6-31G* optimization using the Gaussian03 program[25] on the lowest energy member from each of these groups. The resulting HF energy values and structures were then compared to identify unique complexes. Some of the structures picked from different groups optimized to similar structures, and in total, only two unique structures (dimers A and C) were located. A third dimer configuration (dimer B) was found by enforcing C_s symmetry on the molecule. Without C_s symmetry, this configuration quickly minimizes to dimer C in Figure 1. Finally, Gibbs free energies were obtained using the Gaussian (G3) model chemistry.[26] No further corrections have been made for basis set superposition error, as the method has an inherent correction for basis set artifacts.[27−29]

We started our search for the $HO_2\cdots(H_2O)_2$ complexes by bonding another water molecule to the original $HO_2\cdots H_2O$ complexes in various locations. This resulted in 13 new starting structures. For the exploration of the conformations of these structures, over one hundred additional structures were generated using either a 12-fold or an 8-fold rotation around the hydrogen bond, prior to PM3 optimization of each conformer. The conformers were grouped based on dihedral angles, optimized with HF/6-31G* calculations, grouped based on energies, and the remaining conformers were input to the G3 model chemistry. This approach generated four $HO_2\cdots(H_2O)_2$ complexes. We performed frequency calculations on all complexes using the HF/6-31G* level of theory, and computed a Boltzmann distribution using our G3 model chemistry free energies. All complexes reported have been verified to be stable minima on the HF/6-31G* potential energy surface. All calculations involving hydroperoxy radical were done using spin-unrestricted wave functions.

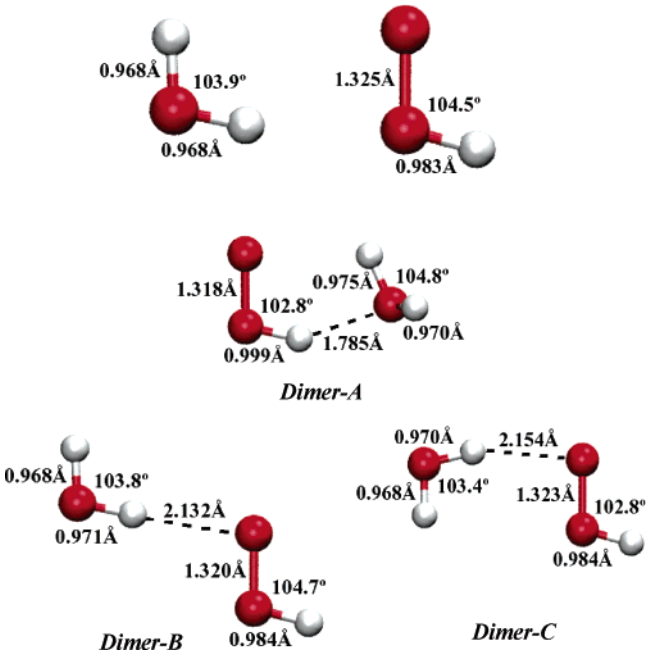

Figure 1. Molecular structures of HO_2, H_2O, and the three $HO_2\cdots H_2O$ dimers determined at the MP2/6-31G* level of theory. Key interatomic distances (angstroms) and angles (degrees) are given.

Results and Discussion

Structures. We found three unique hydrogen bonded complexes of the $HO_2\cdots H_2O$ heterodimer, including the one previously described in the literature where the hydroperoxy radical molecule is the hydrogen bond donor (dimer A in Figure 1). The two new dimer configurations (dimers B and C) both involve the hydroperoxy radical acting as a hydrogen bond acceptor.

Dimer A belongs to the C_1 point group and has an enantiomer. Our MP2(full)/6-31G* optimized value for the hydrogen bond length is 1.785 Å, only 0.004 Å shorter than the MP2/6-311++G(2df,2pd) value of Aloisio and Francisco.[14] The excellent agreement between MP2(full)/6-31G* and MP2/6-311++G(2df,2pd) results allows us to have confidence in the geometries of dimers B and C. Both dimers B and C possess C_s symmetry. Dimer B has a hydrogen bond length of 2.132 Å, indicating weaker attractive forces involved in this dimer formation in comparison to dimer A. Breaking the C_s symmetry in dimer B followed by an optimization forms dimer C, the third and least stable dimer (rotating dimer B's water by 180° results in the formation of dimer C, recapturing C_s symmetry). dimer C has a 2.154 Å hydrogen bond, which is the longest hydrogen bond distance seen in any of the dimer or trimer complexes.

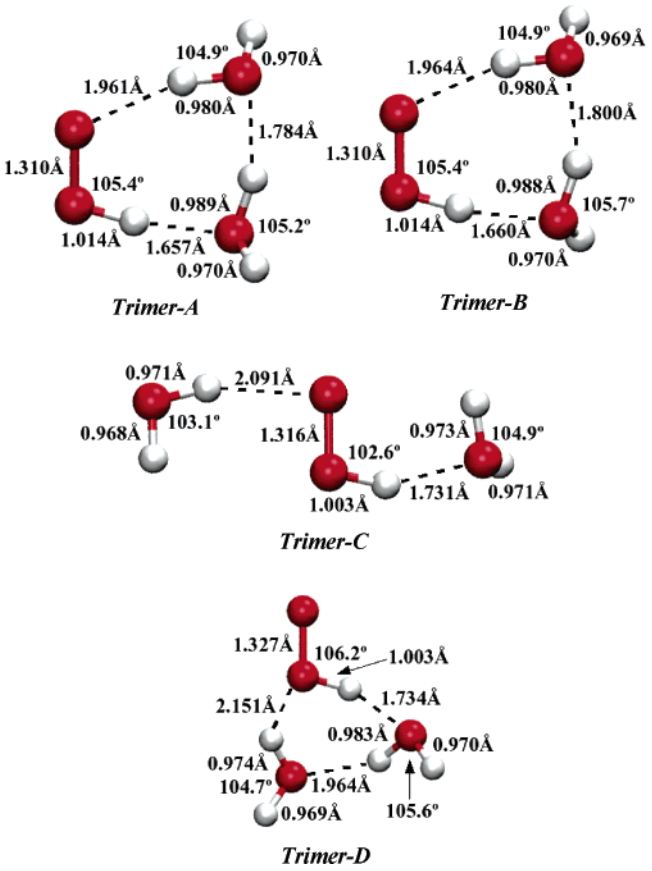

Figure 2. Molecular structures of the four $HO_2\cdots(H_2O)_2$ trimers determined at the MP2/6-31G* level of theory. Key interatomic distances (angstroms) and angles (degrees) are given.

We found four unique configurations for the $HO_2\cdots(H_2O)_2$ trimer complex, all of which have the hydroperoxy radical acting as a hydrogen bond donor and acceptor, as seen in Figure 2. Each trimer possesses C_1 symmetry and has an enantiomer, with trimers A, B, and D existing as cyclic clusters. The only difference between trimers A and B is the orientation of the hydrogen on the water molecules. In these trimers, the cyclic structure allows both oxygens of the hydroperoxy radical to participate in hydrogen bonding with a water, one as a hydrogen bond donor and one as an acceptor. By contrast, in trimer C this is achieved with an extended structure; thus trimer C is the only cluster where the two water molecules do not form a hydrogen bond between each other. Trimer D is unique as the hydroperoxy radical's hydroxyl oxygen acts both as a hydrogen-bond donor and acceptor, while its other oxygen (the radical center) does not participate in any noncovalent interactions. An interesting observation about the trimer complexes is that the hydrogen bonds formed by hydroperoxy radical donating hydrogen are shorter than that observed in dimer A, which has a similar bonding motif. This is an indication that the inclusion of the second water alters the electronic configuration about dimer A, allowing for a more energetically favorable interaction to occur. The cyclic trimers have the same cooperativity interactions as cyclic water clusters that have hydrogen bonds that all donate in the same direction.[24,27,30−40] The most stable $HO_2\cdots(H_2O)_2$ clusters can be constructed simply by replacing one of the water molecules in the most stable water trimers[24] with the radical.

Thermochemistry. As can be seen in Table 1, dimer A is significantly more stable than the two other conformers. For dimer A Aloisio and Francisco reported a CCSD(T)/6-311++G-(2df,2p)//B3LYP/6-311++G(2df,2p) electronic energy for reaction 5, ΔE_{elec}(0 K), of −9.4 kcal·mol^{-1} and after correcting for zero-point vibrational energy, ΔE_{ZPVE}, the energy becomes −6.9 kcal·mol^{-1}.[14] These values are in excellent agreement with our G3 ΔE_{elec}(0 K) and ΔE_{ZPVE} values of −9.1 and −7.1 kcal·mol^{-1}. Including thermal and entropic effects results in dimer A having a enthalpy, $\Delta H°$(298 K), and free energy for reaction 5, $\Delta G°$(298 K), of −7.4 and −0.5 kcal·mol^{-1}. Dimers B and C have a significantly more positive free energy for reaction 5, with values of 2.4 and 3.1 kcal·mol^{-1}. The fact that dimer A consists of two enantiomers further lowers the effective free energy by RT ln(2), for an effective $\Delta G°$(298 K) of −0.94 kcal·mol^{-1}. A Boltzmann calculation, taking into account the enantiomer of dimer A, predicts the relative abundances at 298.15 K of dimers A, B, and C to be 99.5%, 0.4%, and 0.1%. Dimers of hydroperoxy radical and a water molecule will be dominated by dimer A, where the hydroperoxy radical acts as the hydrogen bond donor.

The calculated Gibbs free energy for the reaction forming the two enantiomers of dimer A is −0.9 kcal·mol^{-1}, which is in good agreement with the experimental value of −1.5 (+0.6/−0.3) kcal·mol^{-1} from Kanno and co-workers as determined from their reported equilibrium constant.[12] The relative instability of dimers B and C means that they contribute negligibly to the overall dimer population.

Let us now consider the thermodynamics of the formation of the trimers:

$$HO_2(g) + 2H_2O(g) \rightarrow HO_2\cdots(H_2O)_2(g) \qquad (6)$$

Table 1 contains the energies and the Boltzmann distribution calculation at 298 K for the trimers. As expected based on the strong similarities of their structures, trimers A and B possess nearly the same energy, with $\Delta G°$ (298 K) for reaction 6 of −0.47 and −0.39 kcal·mol^{-1}, respectively. Trimers A and B are also the most stable trimers, and are responsible for 99% of the trimer population. Hydrogen bonding in these two trimers occurs in a three-membered ring, with each molecule/radical acting as both a hydrogen bond donor and acceptor. This cyclic motif has been observed in water clusters,[27,35] and has been attributed to the enhanced cooperativity of these cyclic structures.[37]

We now consider the abundance of these dimers and trimers in the atmosphere at 298 K. This depends on the K_p values for reactions 4 and 5, the abundance of water vapor, and the abundance of hydroperoxy radical:

$$K_{p,dimer} = P_{complex}/P_{HO_2}P_{H_2O} \qquad (7a)$$

$$K_{p,trimer} = P_{complex}/P_{HO_2}(P_{H_2O})^2 \qquad (7b)$$

where P_i are expressed in atmospheres. Since there are multiple dimers and trimers, we compute the ratio $P_{complex,i}/P_{HO_2}$ for each complex i, and determine the fraction of the total HO_2 present as each complex:

$$[P_{complex,i}/P_{HO_2}]/\{1 + \sum_i [P_{complex,i}/P_{HO_2}]\} \qquad (8)$$

Values of K_p calculated from $\Delta G°$(298 K) and accounting for the presence of enantiomers are listed in Table 2. HO_2 concentrations vary enormously in time and space, but often reach 5×10^8 molecules·cm^{-3} in photochemically active regions of the lower troposphere. Present detection methods[41] probably detect $HO_2\cdots H_2O$ and $HO_2\cdots(H_2O)_2$ with roughly the same efficiency as monomer, so we will take 5×10^8 molecules·cm^{-3}

TABLE 1: Changes in G3 Electronic Energies, Enthalpies, Entropies, Gibbs Free Energies, and Boltzmann Distribution for Formation of $HO_2\cdots(H_2O)_n$ for $n = 1$ and 2[a]

$HO_2\cdots(H_2O)_n$	ΔE_{elec}(0 K)	ΔE_{ZPVE}(0 K)	$\Delta H°$(298 K)	$\Delta G°$(298 K)	$\Delta S°$ (cal·mol^{-1}· K^{-1})	distribution (298 K)
$n = 1$						
dimer A	−9.14	−7.06	−7.42	−0.53	76.45	99.5%
dimer B	−3.54	−2.38	−2.15	2.37	84.42	0.4%
dimer C	−3.43	−2.22	−2.04	3.12	82.25	0.1%
$n = 2$						
trimer A	−20.64	−15.80	−16.98	−0.47	89.20	52.5%
trimer B	−20.08	−15.46	−16.52	−0.39	90.45	45.9%
trimer C	−13.53	−10.36	−10.41	1.68	104.04	1.4%
trimer D	−15.71	−11.44	−12.27	2.91	93.66	0.2%

[a] All energies reported are based upon a standard state of 1 atm and have units of kcal·mol^{-1}.

TABLE 2: Equilibrium Constant (Standard State of 1 atm) and Population of Free HO_2 and $HO_2\cdots(H_2O)_n$ for $n = 1$ and 2 at 100% Relative Humidity for Assumed Total [HO_2] $= 5 \times 10^8$ molecules·cm^{-3} at a Temperature of 298.15 K[a]

species	K_p (1 atm)	N (molecules·cm^{-3})
HO_2 monomer		4.3×10^8
$n = 1$		
dimer A (e)	2.4 (13 ± 8)[b]	6.6×10^7
dimer B	0.018	2.5×10^5
dimer C	0.052	6.9×10^4
n = 2		
trimer A (e)	4.4	1.9×10^6
trimer B (e)	3.9	1.6×10^6
trimer C (e)	0.12	4.9×10^4
trimer D (e)	0.015	6.2×10^3

[a] Equilibrium constants are increased by ln 2 for species with two enantiomers, where parenthesis (e) indicates an enantiomeric pair. [b] Reference 12.

to be the concentration of HO_2 (as monomer and in all clusters), and assume that only dimers and trimers contribute significantly to the HO_2 cluster population. For this calculation we will assume a relative humidity (RH) of 100% ($P_{H_2O} = 0.03125$ atm).

Results of these calculations are listed in Table 2. We predict that dimer A will have a concentration of 6.6×10^7 molecules·cm^{-3}, and dimers B and C will have equilibrium concentrations 2−3 orders of magnitude lower. Trimers A and B will have concentrations of 1.9×10^6 and 1.6×10^6 molecules·cm^{-3}, while trimers C and D will have concentrations 1.5−2.5 orders of magnitude lower. Since the hydroperoxy radical concentration is much less than that of water vapor, the computed dimer and trimer concentrations scale linearly with the assumed total HO_2 concentration. Conversely, dimer and trimer concentrations do not scale linearly with RH; decrease of RH to 50% reduces dimer concentrations by 44% and trimer concentrations by 73%.

As noted in the Introduction, one motivation for this study was an interest in how water vapor enhances the self-reaction of HO_2 (reaction 4). The observed effect is roughly linear with water concentration. One commonly used recommendation[7] is that the bimolecular rate constant of reaction 4 is increased by a multiplicative factor:

$$k(T, [H_2O]) = k(T, [H_2O] = 0)\{1 + 1.4 \times 10^{-21}[H_2O]e^{+2200/T}\} \quad (9)$$

where $[H_2O]$ is in molecules·cm^{-3}. It is widely assumed that the increase in rate constant is due to the reaction:

$$HO_2\cdots H_2O(g) + HO_2(g) \rightarrow HOOH(g) + H_2O(g) + O_2(g) \quad (10)$$

If we make the simple assumption that substituting dimer A for HO_2 monomer increases the reaction rate by an enhancement factor, E, due to the fraction, f, of dimer A present, then at 298.15 K eq 9 is related to E and f by

$$\{1 + 1.4 \times 10^{-21}[H_2O]e^{+2200/298.15}\} = (1 - f) + fE \quad (11)$$

The formation of dimer A reduces the concentration of HO_2 monomer by a fraction f, thereby causing a corresponding decrease in the rate of the self-reaction of HO_2 monomer. The $(1 - f)$ term on the right-hand side corresponds to this fractional decrease. We then solve for E using the range of RH used in experiment (0−55%). Using the values of K_p computed here to determine f, we obtain $E = 10.5$. Using Kanno's value of $K_p = 13 \pm 8$, we compute an enhancement factor of 2−10 (4 [+6, −2]).

Vibrational Spectra. The calculated and experimental frequencies for the water and hydroperoxy monomers, and the three dimer complexes are given in Table 3. The scaled HF/6-31G* frequencies for the water monomer agree very well with the experimental frequencies, with a maximum error of 36 cm^{-1}. The frequency of the υ_1 mode of the hydroperoxy monomer should be diagnostic of hydrogen bond donation by HO_2, so it would be helpful to be able to rely on the computed frequencies of this mode in the complexes. Unfortunately, the scaled frequency we obtain at the HF/6-31G* level overestimates the experimental frequency by 172 cm^{-1}.

The experimental OH stretching frequency of the HO_2 molecule in the dimer complex occurs as a strong infrared peak at 3236 cm^{-1}, redshifted by 177 cm^{-1} with respect to hydroperoxy monomer (both in an Ar matrix).[42] Computations indicate a redshift of 101 cm^{-1} for dimer A, but only 3 and 1 cm^{-1} for dimers B and C. Clearly, the redshift seen in the experimental spectrum of the dimer is only consistent with dimer A. Note that the Ar matrix only redshifts υ_1 of hydroperoxy monomer by ∼20 cm^{-1} with respect to the gas-phase value.[43,44]

The scaled vibrational frequencies for the four trimers are reported in Table 4 along with their relative infrared and Raman intensities. The "a" and "d" by the mode labels in Table 4 indicate whether the species involved is acting as a hydrogen bond acceptor or donor in that mode. The intermolecular frequencies all exist below 1000 cm^{-1}, and are complex motions involving two or more of the constituent molecules. Unlike the case of the dimers, it is only within these modes that the trimers exhibit large differences in frequencies between the different conformers, most notably in the H wagging modes.

Detecting these dimer and trimer species is a difficult experimental task because of their low abundance and the potential for their rovibrational spectra to overlap each other's spectra, as well as the spectra of the monomers and pure water clusters. Fortunately, there are a few modes that can be used to distinguish dimer A from trimers A and B. Table 5 summarizes

TABLE 3: Scaled Vibrational Frequencies (cm^{-1}) of HO_2, H_2O, and $HO_2\cdots H_2O$ Complex at HF/6-31G* (Scaled by 0.8929, with Experimental Values in Parentheses and IR and Raman Intensities in Brackets)[a]

mode[b]	H_2O	HO_2	dimer A	dimer B	dimer C
$\upsilon_3(H_2O)$	3740 (3756)[c] (3734)[d]		3730 [m,m] (3691)[f]	3734 [m,m]	3642 [w,s]
$\upsilon_1(H_2O)$	3634 (3657)[c] (3638)[d]		3629 [w,s] (3501.5)[f]	3633 [w,m]	3738 [w,m]
$\upsilon_1(HO_2)$		3585 (3413.0)[e]	3483 [vs,s] (3236.2)[f]	3582 [w,s]	3585 [w,s]
$\upsilon_2(H_2O)$	1631 (1595)[c]		1627 [s,w]	1643 [m,w]	1646 [m,w]
$\upsilon_2(HO_2)$		1449 (1388.9)[e]	1538 [m,w] (1479.3)[f]	1454 [w,w]	1447 [w,w]
$\upsilon_3(HO_2)$		1117 (1100.8)[e]	1126 [w,w] (1120.4)[f]	1125 [w,w]	1117 [w,w]
H wag			562 [s,0]	334 [vs,w]	312 [vs,w]
H···O stretch			332 [s,w]	91.37 [w,0]	136 [0,0]
rock (H_2O)			229 [s,w]	180 [m,w]	136 [m,w]
deformation			207 [w,0]	120 [0,0]	107 [w,w]
deformation			94 [m,w]	37 [0,0]	98 [0,0]
rock (HO_2 and H_2O)			59 [w,0]	34 [m,0]	38 [w,0]

[a] Intensities are listed as very strong (vs), strong (s), medium (m), weak (w), or negligible (0). [b] Mode motion: $\upsilon_1(H_2O)$ for OH symmetric stretching in H_2O; $\upsilon_2(H_2O)$ for HOH bending in H_2O; $\upsilon_3(H_2O)$ for OH asymmetric stretching in H_2O; $\upsilon_1(HO_2)$ for H−O stretching in HO_2; $\upsilon_2(HO_2)$ for HOO bending in HO_2; $\upsilon_3(HO_2)$ for O−O stretching in HO_2. [c] Reference 46. [d] Reference 47. [e] Reference 48. [f] Reference 49.

TABLE 4: Scaled Vibrational Frequencies (cm^{-1}) of $HO_2\cdots(H_2O)_2$ Complexes at HF/6-31G* (Scaled by 0.8929, with IR and Raman Intensities in Brackets[a])

mode[a]	trimer A	trimer B	trimer C	trimer D
$\upsilon_3(H_2O$ d)	3717 [m,m]	3721 [m,m]	3733 [w,s]	3722 [m,m]
$\upsilon_1(H_2O$ a)	3532 [s,s]	3544 [s,s]	3732 [m,s]	3561 [s,s]
$\upsilon_1(H_2O$ d)	3610 [m,s]	3613 [m,s]	3642 [w,s]	3617 [w,s]
$\upsilon_3(H_2O$ a)	3702 [m,m]	3706 [m,m]	3632 [w,s]	3709 [m,m]
$\upsilon_1(HO_2)$	3373 [vs,vs]	3379 [vs,vs]	3455 [vs,vs]	3430 [vs,s]
$\upsilon_2(H_2O$ d)	1637 [m,w]	1635 [m,w]	1652 [s,m]	1636 [w,w]
$\upsilon_2(H_2O$ a)	1649 [m,w]	1656 [m,w]	1626 [m,w]	1649 [m,w]
$\upsilon_2(HO_2)$	1568 [m,w]	1570 [m,w]	1536 [w,vw]	1512 [m,w]
$\upsilon_3(HO_2)$	1139 [w,w]	1139 [w,w]	1128 [w,vw]	1127 [w,w]
H wag	721 [m,w]	646 [m,w]	621 [m,0]	711 [w,0]
H wag	665 [m,0]	659 [m,w]	334 [m,vw]	570 [vs,w]
H wag (H_2O a, d)	455 [m,w]	403 [m,0]	297 [w,vw]	390 [s,w]
O···O stretch (H_2O a, HO_2)	263 [m,w]	240 [w,0]	234 [m,vw]	212 [w,0]
H wag	355 [m,w]	262 [m,w]	215 [m,0]	346 [m,0]
H twist (H_2O d)	246 [w,w]	384 [m,w]	140 [w,vw]	242 [w,0]
rock (H_2O a & d)	229 [w,0]	197 [w,w]	130 [w,0]	193 [m,w]
O···O stretch (H_2O a & d)	199 [w,0]	191 [w,w]	112 [w,0]	172 [w,0]
hydrogen motion	164 [m,w]	133 [m,0]	65 [w,0]	103 [m,w]
hydrogen motion	65 [w,0]	54 [w,w]	47 [w,vw]	124 [w,0]
heavy atom motion	151 [w,w]	156 [w,w]	25 [w,0]	36 [w,0]
heavy atom motion	104 [w,0]	100 [w,0]	22 [w,0]	87 [w,w]

[a] See Table 3 for description of intensities and mode motion.

TABLE 5: HF/6-31G* Scaled Infrared and Raman Absorptions for the Low Energy Clusters $HO_2\cdots(H_2O)_n$ for $n = 1$ and 2, along with the Respective Monomers[a]

modes	HO_2	H_2O	$H_2O\cdots H_2O$[b]	$H_2O\cdots(H_2O)_2$[b]	dimer A	trimer A	trimer B
υ_1 (H_2O)		3634 [m, na]	3630 [m,w]	3562 [s,m]; 3558 [s,m]; 3519 [w,s]	3629 [w,s] (−5//na)	3532 [s,s] (−102//−97)	3544 [s,s] (−90//+12)
υ_1 (HO_2)	3585 [m, na]				3483 [vs,s] (−102//na)	3373 [vs,vs] (−212//−110)	3379 [vs,vs] (−206//+6)
H motion						721 [m,w]	646 [m,w] (na//−75)
						665 [m,0]	659 [m,w] (na//−19)
			553 [m,w]	598 [s,w]	562 [s,0]	455 [m,w] (na//−107)	403 [m,0] (na//−52)
			342 [m,w]	407 [m,w]; 314 [w,w]; 296 [w,w]; 221 [w,w]		355 [m,w]	262 [m,w] (na//−93)

[a] In parentheses is given the spectral shift from the monomer//shift from the preceding cluster, where a positive value indicates a blue shift and a negative value indicates a red shift. [b] Reference 45.

this information, showing that dimer A's hydroperoxy radical's O−H stretch will be red shifted by approximately 100 cm^{-1} from that of free hydroperoxy and will have a very intense infrared peak. Trimers A and B will have this mode, further red shifted by another 100 cm^{-1}, again with very strong infrared absorption bands. Similarly, water's symmetric O−H stretch in dimer A will be unchanged from that of free water, but if trimers A or B form, a strong infrared peak will appear red shifted by approximately 100 cm^{-1}. In terms of the symmetric O−H stretching mode of the water molecule ($\upsilon_1(H_2O)$) and hydrogen wagging mode of the complex, the unique infrared peaks for dimer A and trimers A and B will be masked by vibrational modes that arise from the formation of the $H_2O\cdots H_2O$ and $H_2O\cdots(H_2O)_2$ complexes,[45] as seen in Table 5.

Conclusion

Our thorough search of conformational space discovered two unique $HO_2\cdots H_2O$ complexes in which hydroperoxy acts as a hydrogen bond acceptor, in addition to the previously described $HO_2\cdots H_2O$ complex in which hydroperoxy acts as a hydrogen bond donor. The donor complex is the most abundant of the three, resulting from a more favorable free energy of formation

for the two enantiomers of this complex. Our computed binding energies and free energies were very similar to those obtained from previous computations. Our free energy of formation is well within the error bars of the experimental value. We identified two cyclic trimers that are very similar in energy. The most favorable hydrogen-bonding motif has both hydroperoxy radical's oxygens participating in hydrogen bonding, one as a hydrogen bond donor and the other as an acceptor, with the waters forming a hydrogen bond between them. This same motif has been observed in cyclic water clusters,[27,35] and has been attributed to the enhanced cooperativity of these cyclic structures.[37] We predict that when the HO_2 concentration is on the order of 10^8 molecules·cm^{-3} in the lower troposphere at 298 K, that the number of $HO_2\cdots H_2O$ complexes is on the order of 10^7 molecules·cm^{-3} and the number of $HO_2\cdots(H_2O)_2$ complexes is on the order of 10^6 molecules·cm^{-3}.

Acknowledgment. Acknowledgment is made to the donors of the Petroleum Research Fund, administered by the American Chemical Society, to the Research Corporation, to NIH, to DOD, and to Hamilton College for support of this work. This project was supported in part by NSF Grant CHE-0457275, and by NSF Grants CHE-0116435 and CHE-0521063 as part of the MERCURY high-performance computer consortium (http://mercury.chem.hamilton.edu). T.S.D. would like to acknowledge support from the National Science Foundation under Grant ATM-0352926.

Supporting Information Available: Tables containing energy values and coordinates from the final orientation for dimer A, dimer B, dimer C, trimer A, trimer B, trimer C, trimer D, water, and HO_2 radical. This material is available free of charge via the Internet at http://pubs.acs.org.

References and Notes

(1) Wayne, R. P. *Chemistry of Atmospheres*, 2nd ed.; Oxford University Press: Oxford, U.K., 1991.
(2) Sander, S. P.; Peterson, M.; Watson, R. T.; Patrick, R. *J. Phys. Chem.* **1982**, *86*, 1236.
(3) Hamilton, J. E., Jr.; Lii, R.-R. *Int. J. Chem. Kinet.* **1977**, *9*, 875.
(4) DeMore, W. B. *J. Phys. Chem.* **1979**, *83*, 1113.
(5) Cox, R. A.; Burrows, J. P. *J. Phys. Chem.* **1979**, *83*, 2560.
(6) Lii, R.-R.; Sauer, J.; Myran, C.; Gordon, S. *J. Phys. Chem.* **1981**, *85*, 2833.
(7) Kircher, C. C.; Sander, S. P. *J. Phys. Chem.* **1984**, *88*, 2082.
(8) Hamilton, J. E., Jr.; Naleway, C. A. *J. Phys. Chem.* **1976**, *80*, 2037.
(9) Pan, X.; Bass, A. D.; Jay-Gerin, J.-P.; Sanche, L. *Icarus* **2004**, *172*, 521.
(10) Baragiola, R. A. *Nucl. Instrum. Methods Phys. Res. Sect. B−Beam Interact. Mater. At.* **2005**, *232*, 98.
(11) De Grey, A. *DNA Cell Biol.* **2002**, *21*, 251.
(12) Kanno, N.; Tonokura, K.; Tezaki, A.; Koshi, M. *J. Phys. Chem. A* **2005**, *109*, 3153.
(13) Aloisio, S.; Francisco, J. S.; Friedl, R. R. *J. Phys. Chem. A* **2000**, *104*, 6597.
(14) Aloisio, S.; Francisco, J. S. *J. Phys. Chem. A* **1998**, *102*, 1899.
(15) Zhu, R. S.; Lin, M. C. *Chem. Phys. Lett.* **2002**, *354*, 217.
(16) Belair, S. D.; Kais, S.; Francisco, J. S. *Mol. Phys.* **2002**, *100*, 247.
(17) Lendvay, G. *Z. Phys. Chem.-Int. J. Res. Phys. Chem. Chem. Phys.* **2001**, *215*, 377.
(18) Zhu, R. S.; Lin, M. C. *Physchemcomm* 2001.
(19) Zhu, R. S.; Lin, M. C. *Physchemcomm* **2003**, *6*, 51.
(20) Shi, Q. C.; Belair, S. D.; Francisco, J. S.; Kais, S. *Proc. Natl. Acad. Sci. U.S.A.* **2003**, *100*, 9686.
(21) Sennikov, P. G.; Ignatov, S. K.; Schrems, O. *Chemphyschem* **2005**, *6*, 392.
(22) Hansen, J. C.; Francisco, J. S. *Chemphyschem* **2002**, *3*, 833.
(23) SPARTAN. Spartan; 5.1.3 ed.; Wavefunction, Inc.: Irvine, CA 92612, 1998.
(24) Day, M. B.; Kirschner, K. N.; Shields, G. C. *J. Phys. Chem. A* **2005**, *109*, 6773.
(25) Frisch, M. J.; Trucks, G. W.; Schlegel, H. B.; Scuseria, G. E.; Robb, M. A.; Cheeseman, J. R.; Montgomery, J. A., Jr.; Vreven, T.; Kudin, K. N.; Burant, J. C.; Millam, J. M.; Iyengar, S. S.; Tomasi, J.; Barone, V.; Mennucci, B.; Cossi, M.; Scalmani, G.; Rega, N.; Petersson, G. A.; Nakatsuji, H.; Hada, M.; Ehara, M.; Toyota, K.; Fukuda, R.; Hasegawa, J.; Ishida, M.; Nakajima, T.; Honda, Y.; Kitao, O.; Nakai, H.; Klene, M.; Li, X.; Knox, J. E.; Hratchian, H. P.; Cross, J. B.; Bakken, V.; Adamo, C.; Jaramillo, J.; Gomperts, R.; Stratmann, R. E.; Yazyev, O.; Austin, A. J.; Cammi, R.; Pomelli, C.; Ochterski, J. W.; Ayala, P. Y.; Morokuma, K.; Voth, G. A.; Salvador, P.; Dannenberg, J. J.; Zakrzewski, V. G.; Dapprich, S.; Daniels, A. D.; Strain, M. C.; Farkas, O.; Malick, D. K.; Rabuck, A. D.; Raghavachari, K.; Foresman, J. B.; Ortiz, J. V.; Cui, Q.; Baboul, A. G.; Clifford, S.; Cioslowski, J.; Stefanov, B. B.; Liu, G.; Liashenko, A.; Piskorz, P.; Komaromi, I.; Martin, R. L.; Fox, D. J.; Keith, T.; Al-Laham, M. A.; Peng, C. Y.; Nanayakkara, A.; Challacombe, M.; Gill, P. M. W.; Johnson, B.; Chen, W.; Wong, M. W.; Gonzalez, C.; Pople, J. A. *Gaussian 03*, revision C.02. Gaussian, Inc.: Wallingford, CT, 2004.
(26) Curtiss, L. A.; Raghavachari, K.; Redfern, P. C.; Rassolov, V.; Pople, J. A. *J. Chem. Phys.* **1998**, *109*, 7764.
(27) Dunn, M. E.; Pokon, E. K.; Shields, G. C. *J. Am. Chem. Soc.* **2004**, *126*, 2647.
(28) Pickard, F. C.; IV; Dunn, M. E.; Shields, G. C. *J. Phys. Chem. A* **2005**, *109*, 4905.
(29) Pickard, F. C.; IV; Pokon, E. K.; Liptak, M. D.; Shields, G. C. *J. Chem. Phys.* **2005**, *024302*.
(30) Tsai, C. J.; Jordan, K. D. *J. Phys. Chem.* **1993**, *97*, 5208.
(31) Xantheas, S. S. *J. Chem. Phys.* **1994**, *100*, 7523.
(32) Xantheas, S. S. *J. Chem. Phys.* **1995**, *102*, 4505.
(33) Gruenloh, C. J.; Carney, J. R.; Arrington, C. A.; Zwier, T. S.; Fredericks, S. Y.; Jordan, K. D. *Science* **1997**, *276*, 1678.
(34) Ugalde, J. M.; Alkorta, I.; Elguero, J. *Angew. Chem., Int. Ed.* **2000**, *39*, 717.
(35) Dunn, M. E.; Pokon, E. K.; Shields, G. C. *Int. J. Quantum Chem.* **2004**, *100*, 1065.
(36) Day, M. B.; Kirschner, K. N.; Shields, G. C. *Int. J. Quantum Chem.* **2005**, *102*, 565.
(37) Xantheas, S. S. *NATO ASI Series, Ser. C: Math. Phys. Sci.* **2000**, *561*, 119.
(38) Keutsch, F.; Saykally, R. J. *Proc. Natl. Acad. Sci. U.S.A.* **2001**, *98*, 10533.
(39) Xantheas, S. S.; Burnham, C. J.; Harrison, R. J. *J. Chem. Phys.* **2002**, *116*, 1493.
(40) Ohno, K.; Okimura, M.; Akai, N.; Katsumoto, Y. *PCCP Phys. Chem. Chem. Phys.* **2005**, *7*, 3005.
(41) Heard, D. E.; Pilling, M. J. *Chem. Rev.* **2003**, *103*, 5163.
(42) Milligan, D. E.; Jacox, M. E. *J. Chem. Phys.* **1963**, *38*, 2627.
(43) Yamada, C.; Endo, Y.; Hirota, E. *J. Chem. Phys.* **1983**, *78*, 4379.
(44) Thompson, W. E.; Jacox, M. E. *J. Chem. Phys.* **1989**, *91*, 3826.
(45) Dunn, M. E.; Evans, T. M.; Kirschner, K. N.; Shields, G. C. *J. Phys. Chem. A* **2005**, *110*, 303.
(46) Fraley, P. E.; Narahari-Rao, K. *J. Mol. Spectrosc.* **1969**, *29*, 348.
(47) Engdahl, A.; Nelander, B. *J. Mol. Struct.* **1989**, *193*, 101.
(48) Jacox, M. E. *J. Phys. Chem. Ref. Data* **1994**, 1.
(49) Nelander, B. *J. Phys. Chem. A* **1997**, *101*, 9092.